



LUND UNIVERSITY

Radioactivity Exploration from the Arctic to Antarctica. Part 5: The Tundra-94 expedition

Persson, Bertil R; Holm, Elis; Josefsson, Dan; Carlsson, Kjell-Åke

Published in:
Acta Scientiarum Lundensia

DOI:
[10.13140/RG.2.1.5115.0807](https://doi.org/10.13140/RG.2.1.5115.0807)

2015

[Link to publication](#)

Citation for published version (APA):

Persson, B. R., Holm, E., Josefsson, D., & Carlsson, K.-Å. (2015). Radioactivity Exploration from the Arctic to Antarctica. Part 5: The Tundra-94 expedition. *Acta Scientiarum Lundensia*, 2015(006), 1-20.
<https://doi.org/10.13140/RG.2.1.5115.0807>

Total number of authors:
4

General rights

Unless other specific re-use rights are stated the following general rights apply:
Copyright and moral rights for the publications made accessible in the public portal are retained by the authors and/or other copyright owners and it is a condition of accessing publications that users recognise and abide by the legal requirements associated with these rights.

- Users may download and print one copy of any publication from the public portal for the purpose of private study or research.
- You may not further distribute the material or use it for any profit-making activity or commercial gain
- You may freely distribute the URL identifying the publication in the public portal

Read more about Creative commons licenses: <https://creativecommons.org/licenses/>

Take down policy

If you believe that this document breaches copyright please contact us providing details, and we will remove access to the work immediately and investigate your claim.

LUND UNIVERSITY

PO Box 117
221 00 Lund
+46 46-222 00 00



Volume ASL 2015-006

Citation: (Acta Scientiarum Lundensia)

PERSSON, B. R. R., HOLM, E., JOSEFSSON, D. & CARLSSON, K.-Å. (2015) Radioactivity Exploration from the Arctic to Antarctica. Part 5: The Tundra-94 expedition, *Acta Scientiarum Lundensia*, Vol. 2015-006, pp.1-20. ISSN 1651-5013, DOI: 10.13140/RG.2.1.5115.0807.

Corresponding author:

Bertil R.R. Persson, PhD. MDhc, professor emeritus
Lund University, Dept. of medical radiation physics,
Barnågatan 2, S-22185 Lund Sweden
E-mail: bertil_r.persson@med.lu.se

Radioactivity Exploration from the Arctic to Antarctica. Part 5: The Tundra-94 expedition

Bertil R.R. Persson, Elis Holm¹⁾, Dan Josefsson²⁾, and Kjell-Åke Karlsson

Lund University, Dept. of medical radiation physics, S-22185 Lund Sweden

¹⁾Present address: Dept. of Radiation Physics, University of Gothenburg, SE-41345 Gothenburg, Sweden.

²⁾ Present address: Department of Medical and Health Sciences, Linköping University, SE-581 83 Linköping, Sweden

Abstract

The joint Swedish-Russian “*Tundra Ecology-94*” expedition during 1994 used the large Russian ice-breaking research vessel R/V Akademik Fedorov a platform and went along a coastline of 3500 km-from the Kola Peninsula 10°E to Kolyuchinskaya Bay 173°E. Radioactivity in air, seawater and sediment was explored at various locations along the route.

The average of ⁷Be activity concentration in air over the Arctic Ocean was found to be only about 0.6 mBq.m⁻³, in air close to the Siberian coast-line, however, it was as high as 11 mBq.m⁻³. The activity concentration of ²¹⁰Pb in the air over the Arctic Ocean varies between 37 – 176 μBq.m⁻³. In the air close to the Siberian coastline 71°N 84°E, however, the activity concentration of ²¹⁰Pb in the air was much higher, about 2500 μBq.m⁻³.

Anthropogenic radioactivity in the Arctic originate from nuclear weapons fallout, release from nuclear fuel reprocessing plant, and from the Chernobyl accident. The minimum values of the ¹³⁷Cs activity concentration water along the route of the Tundra were found in South-eastern Barents Sea: 5.3 Bq.m⁻³ of surface-water, and of bottom-water 6.4 Bq.m⁻³. Maximum values were found in the Western Laptevsea: 12.8 Bq.m⁻³ of surface-water, and of bottom-water 5.1 Bq.m⁻³. East of 150 °E the ¹³⁴Cs / ¹³⁷Cs ratios are less than 0.003, indicating that less than 6% of the ¹³⁷Cs originated from the Chernobyl accident.

¹³⁷Cs levels are reduced to values of about 1.4 Bq.m⁻³ in the low salinity water near the mouths of the Ob and Yenisey Rivers. The ¹³⁴Cs / ¹³⁷Cs activity ratio of 0.014 in the freshwater indicates that the Chernobyl component in the river systems is the same (30%) as in the marine waters west of 150 °E.

In surface water the ⁹⁰Sr activity concentration range from 2 to 4 Bq.m⁻³, Maximum values about 3.5 Bq.m⁻³ were found between 100-140 °E. But east of 150 °E the values decreased to about 0.5 Bq.m⁻³ at 170 °E. In bottom water the ⁹⁰Sr activity concentration range from 1.5 at 40 °E to maximum values about 4 Bq.m⁻³ between 100-120 °E. The measured ⁹⁰Sr/¹³⁷Cs ratios in surface water close to a value of 0.14 over a wide range of stations from the Barents to the Laptev Seas. The ¹²⁹I concentration in sea-water along the route of the Tundra expedition decrease from about 20·10¹¹ atoms.l⁻¹ at 40 °E, to about 1·10¹¹ atoms.l⁻¹ east of 160 °E.

The ²³⁹⁺²⁴⁰Pu activity concentration in surface seawater decrease from about 10 mBq.m⁻³ to about 1 mBq.m⁻³ east of 160 °E. In bottom seawater it is more evenly distributed between 10⁻⁴ mBq.m⁻³, with minimum at 60-80 °E and maxima at 40°E and 160 °E. Measured ²³⁸Pu/^{239,240}Pu activity ratios in the water column yield no evidence of any leakage of plutonium from dumped nuclear wastes in the Kara and Barents Seas.

Keywords: *Tundra Ecology-94*, Akademik Fedorov, ⁷Be, air, Arctic Ocean, Siberian coast-line, ¹³⁷Cs, ¹³⁴Cs / ¹³⁷Cs-ratio, Chernobyl accident, surface water, ⁹⁰Sr, ¹²⁹I, ²³⁹⁺²⁴⁰Pu, ²³⁸Pu/^{239,240}Pu-activity ratio,

A. Introduction

The joint Swedish-Russian “*Tundra Ecology-94*” expedition during 1994 along a coastline of 3500 km-from the Kola Peninsula 10°E to Kolyuchinskaya Bay 173°E, used the large Russian ice-breaking research vessel R/V Akademik Fedorov a platform (**Figure 5-1**). In **Table 5-1** is given locations of the various places where we were transferred a shore with helicopters (**Figure**

5-6) or escorted by on Russian atomic Icebreaker (**Figure 5-2**). In **Figure 5-3** is given a diagram of the route of the expedition.



Figure 5-1a.

R/V Akademik Fedorov in the harbour of Gothenburg loading of the Tundra-94 expedition



Figure 5-1b.

R/V Akademik Fedorov, ready to leave for the Arctic

Table 5-1

Expedition route and research sites of the "Tundra Ecology-94" expedition

Visiting date 1	On return date 2	Site No.	Name	Position
06-04	09-08		Gothenburg	57.43°N 11.98°E
06-08>>09	09-02		Murmansk	68.57°N 44.10°E
06-10	08-31	1(27)	Kachkovsky Bay. Kola Peninsula	67.30°N 41.00°E
06-12>>13	08-29>>30	2(26)	North-Eastern Kanin Peninsula	68.15°N 6.00°E
06-14>>15	08-26>>28	3(25)	Kolguev Island	69.15°N 50.00°E
06-15>>16	08-25>>26	4(24)	Pechora Bay	68.5°N 54.00°E
06-17>>20	08-22>>08-23	5(23)	Western Yamal Peninsula	70.45°N 67.00°E
06-21>>22	08-20>>21	6 (22)	Belyi Island. Northern Yamal Peninsula	73.00°N 70.00°E
06-22>>23	08-18>>19		Dickson	
06-23		7	Arctic Institute Islands	75.00°N. 82.00°E
06-24>>26	08-15>>17	8(21)	North West of Taymyr Peninsula	76.00°N 94.00°E
06-27>>28	08-13>>14	9(20)	Chelyuskin Peninsula	77.20°N 102.00°E
08-29>>30	08-10>>11	10(19)	North-east of Taymyr Peninsula	76.00°N 112.00°E
07-03>>05			Khatanga rotation point 1	74.00°N 110.00°E
07-05>>06		11	Olenekskiy Bay	73.15°N 120.00°E
	08-08>>08-08		Tiksi rotation point 2	74.00°N 110.00°E
	08-03>>08-04	12	Yana Delta	71.30°N 136.00°E
07-10>>11	07-31>>08-02	13	New Siberian Islands	75.00°N 140.00°E
07-14>>15		14	Lopatka Peninsular, N-W Indigirka	71.45°N 149.00°E
07-17>>18		15	North-east of Kolyma Delta	71.45°N 158.00°E
07-20>>21		16	Ayon Island	69.50°N 168.00°E
07-22>>26		17	South-western Wrangels Island	70.50°N 179.00°E
07-25	point of return	18	Kolyuchinskaya Bay	67.00°N 173.45°E



Figure 5-2.
The Russian atomic icebreaker approaching To assist Akademik Fedorov in the heavy ice.

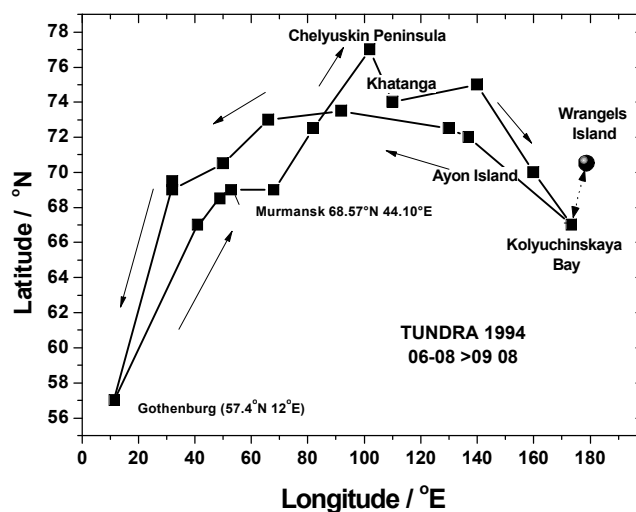


Figure 5-3.
Route of the Tundra-94 expedition with R/V Akademik Fedorov along the Siberian Coastline, with a helicopter tour to Wrangles Island.

B. Material and Methods.

B1. Air sampling

Air filter samples were taken by using an Andersen sampler with the capacity of $100 \text{ m}^3\text{h}^{-1}$ (filter size $0.25 \times 0.25 \text{ m}$ membrane filter). An air volume of about $1\,500 \text{ m}^3$ were collected at a

rate of $100 \text{ m}^3\text{h}^{-1}$ during each sampling occasion. The Andersen sampler was placed close together with a FOA transportable reference high volume air sampler (filter size $0.56 \times 0.56 \text{ m}$, microsorban filter, $100 \text{ m}^3\text{h}^{-1}$), previously taken part in an inter calibration of samplers (Vintersved, 1994). The filters were stored on board and then taken the institute at Lund for analysis. The results of the Anderson sampler were normalized to those of the calibrated FOA sampler based on ^7Be measurements. FOA nowadays FOI, is a Swedish research institute in the areas of defence and security.



Figure 5-4.
The FOA air sampler

B2. Analysis of the air filters

The filters were measured for ^7Be by gamma spectrometry using a high performance Germanium detector (HpGe Canberra). After adding ^{209}Po as radiochemical yield determinant, the samples were wet-ashed by using a mixture of concentrated nitric and per-chloric acids. Polonium was spontaneously deposited on nickel discs, and measured by alpha spectrometry, using surface ion implanted silicon detectors.

Remaining traces of polonium, were removed by anion exchange. The solution was then stored for about 8 months to allow equilibrium in-growth of ^{210}Po from ^{210}Pb . The activity of ingrown ^{210}Po , was then analysed as described above, and finally the activity concentrations of ^{210}Po and ^{210}Pb in air were calculated.

B3. Water sampling

Large volume (200 litre) water samples, were taken from the water cooling system of the ship, and collected in special vessels for precipitation of ^{137}Cs and $^{239+240}\text{Pu}$. Continuous sampling of caesium also took place with a separate pump and a pipe hanging from the rail of the ship to about 2 m depth. An in-line system with filters impregnated with Copper-Ferro-Cyanide ($\text{Cu}_2\text{Fe}(\text{CN})_6$) was used to collect Caesium isotopes from the seawater. The filters were dried and brought to Lund for radiochemical analysis. After ashing the filters at $420 \text{ }^\circ\text{C}$, the residues were analysed for ^{134}Cs and ^{137}Cs by using a Ge (Li) gamma spectrometer.



Figure 5-5.

Interior of the water laboratory container, with the two 200 litre precipitation vessels to the right and the cartridge filters on the wall to the left



Figure 5-6.

Bertil Persson and Kjell-Åke Carlsson landed on the tundra after a tour with the Russian helicopter in the back.



Figure 5-6a.
View of the tundra

Figure 5-6b.
Sampling of the tundra

Figure 5-6a.
Closer view



Figure 5-7a.
Chelyuskin Peninsula 77.20°N; 102.00°E
Summer lake of the waste accumulated during the winter.



Figure 5-7a.
Road at Chelyuskin Peninsula



Figure 5-7a.
A mound of flat stones raised by Adolf Erik Nordenskiöld's expedition in 1878 as a memorial of the visit.



Figure 5-7b.
An anchor left by Adolf Erik Nordenskiöld's expedition in 1878.

C. Results

C1. ^{210}Pb and ^7Be in air 1994- June 08 > September 08

In the **Figures 5-8a** and **b** are given the activity concentrations of ^{210}Pb ($\mu\text{Bq}\cdot\text{m}^{-3}$), and ^7Be ($\text{mBq}\cdot\text{m}^{-3}$) in air, measured during 1994-June 8 < September 8 at the joint Swedish-Russian Tundra Ecology-94 expedition.

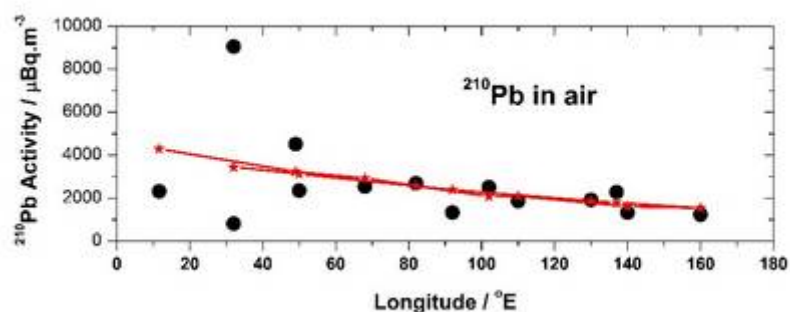


Figure 5-8 a

Longitudinal distribution of ^{210}Pb air concentration ($\mu\text{Bq}\cdot\text{m}^{-3}$) during 1994-June 8 < September 8 at the Tundra Ecology-94 expedition. Predicted values in read.

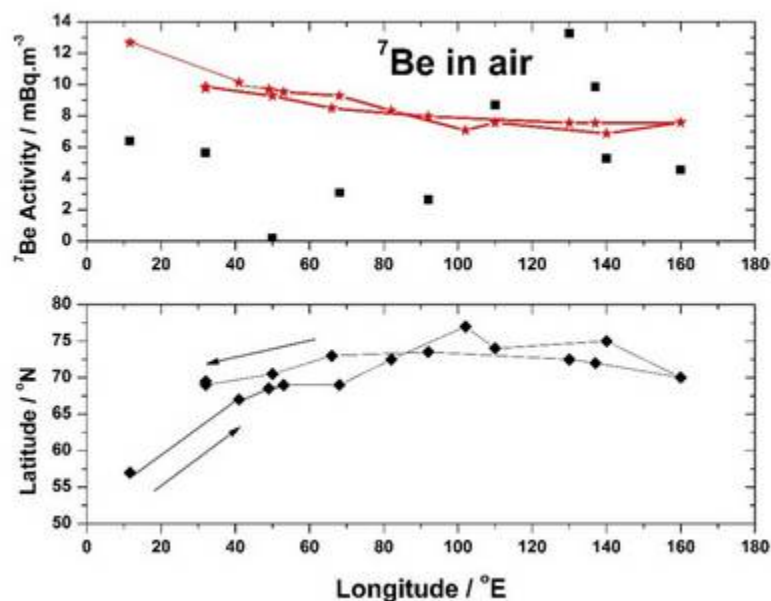


Figure 5-8 b Longitudinal distribution of ^7Be air concentration ($\text{mBq}\cdot\text{m}^{-3}$) during 1994-June 8 < September 8 and the route of the Tundra Ecology-94 expedition. Predicted values in read.

Equations of the PLS models for the air concentrations displayed in red in Figure 5-8:

$$C_{7\text{Be}} = 24.65 - 0.207 \cdot \text{Latitude} - 0.016 \cdot \text{Longitude}; [\text{mBq}\cdot\text{m}^{-3}]$$

Goodness of fit statistics (Variable $C_{7\text{Be}}$): $R^2 = 0.036$

$$C_{210\text{Pb}} = 6992 - 44.45 \cdot \text{Latitude} - 14.61 \cdot \text{Longitude}; [\mu\text{Bq}\cdot\text{m}^{-3}]$$

Goodness of fit statistics (Variable $C_{210\text{Pb}}$): $R^2 = 0.176$

Table 5-2a

Average air concentrations of ^7Be and ^{210}Pb measured during 1994-June 8 > September 8 at the joint Swedish-Russian Tundra Ecology-94 expedition.

Isotope	Date	Average	SD	SE	
Latitude		71	4	1	N
Longitude		84	47	11	E
^7Be	1994-0605 > 0719	11.4	9.0	3.2	mBq/m ³
^{210}Pb	1994-0605 > 0719	2373	1029	364	μBq/m ³
^7Be	1994-07-19 > 0908	7.2	5.4	2.0	mBq/m ³
^{210}Pb	1994-07-19 > 0908	2712	2854	1079	μBq/m ³

During the Swedish-Russian Tundra Ecology-94 expedition along the Siberian coastline, the average air concentrations of ^7Be and ^{210}Pb measured during May-July were 11 ± 3 and 2.4 ± 0.4 mBq.m⁻³ respectively and during July-September they were 7.2 ± 2 and 2.7 ± 1.1 mBq.m⁻³ respectively.

Table 5-2 b

Ratios of average air concentrations of ^7Be and ^{210}Pb measured during 1994-June 8 > September 8 at the joint Swedish-Russian Tundra Ecology-94 expedition.

Isotope ratio	Date	Average	SE
Latitude		71	1
Longitude		84	11
$^7\text{Be} / ^{210}\text{Pb}$	1994-0605 > 0719	5	2
$^7\text{Be} / ^{210}\text{Pb}$	1994-07-19 > 0908	3	1

C2. ^{137}Cs activity concentration in seawater

The ^{137}Cs activity concentration water along the route of the Tundra expedition is shown in **figures 5-9a** and **b** respectively. The minimum values were found in South-Eastern Barents Sea: 5.3 Bq.m⁻³ of surface-water, and of bottom-water 6.4 Bq.m⁻³. Maximum values were found in the Western Laptevsea: 12.8 Bq.m⁻³ of surface-water, and of bottom-water 5.1 Bq.m⁻³.

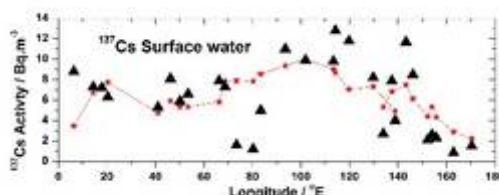


Figure 5-9a. Longitudinal distribution of ^{137}Cs activity concentration in surface seawater along the route of Tundra expedition. Predicted values in read

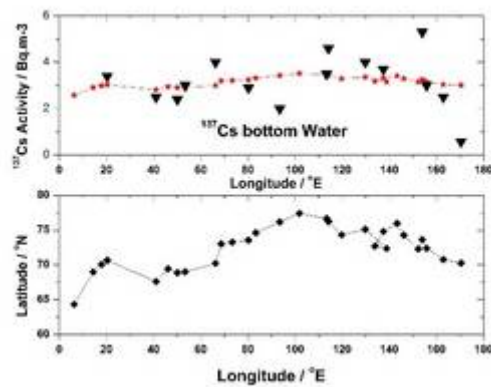


Figure 5-9b. Longitudinal distribution of ^{137}Cs activity concentration in bottom seawater and the route of Tundra expedition. Predicted values in red

Equation of the PLS model for activity concentration in surface water (SW), displayed in red in **Figure 5-9**:

$$^{SW}\text{C}_{137\text{Cs}} = -44.93 + 0.756 \cdot (\text{Latitude}^\circ\text{N}) - 0.035 \cdot (\text{Longitude}^\circ\text{E}); [\text{Bq}\cdot\text{m}^{-3}]$$

Goodness of fit statistics : $R^2 = 0,312$

Equation of the PLS model for bottom water (BW):

$$^{BW}\text{C}_{137\text{Cs}} = -2.005 + 0.071 \cdot (\text{Latitude}^\circ\text{N}) + 4,49 \cdot 10^{-5} \cdot (\text{Longitude}^\circ\text{E}); [\text{Bq}\cdot\text{m}^{-3}]$$

Goodness of fit statistics (Variable $^{BW}\text{C}_{137\text{Cs}}$ bottom water): $R^2 = 0,076$



Figure 5-10a.
View of the Arctic sea



Figure 5-10b.
View of the Arctic sea



Figure 5-10c.
View of the Arctic sea

C3. $^{134}\text{Cs}/^{137}\text{Cs}$ activity ratio in sea water

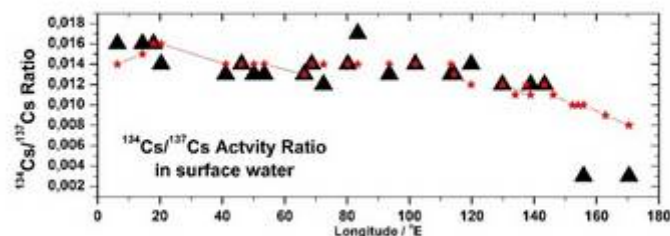


Figure 5-11a.
Longitudinal distribution of $^{134}\text{Cs}/^{137}\text{Cs}$ activity ratio in surface sea-water along the route of Tundra expedition. Predicted values in red

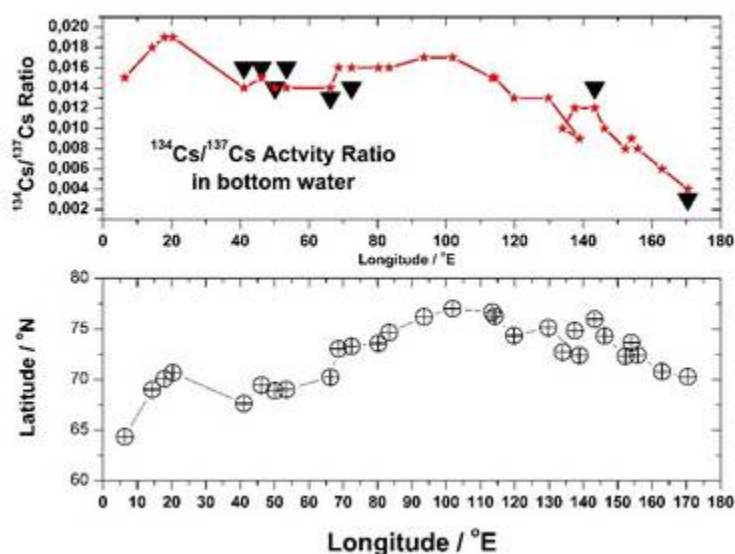


Figure 5-11b. Longitudinal distribution of $^{134}\text{Cs}/^{137}\text{Cs}$ activity ratio in bottom sea water along the route of Tundra expedition. Predicted values in read

Equation of the PLS model for $^{134}\text{Cs}/^{137}\text{Cs}$ ratio in surface water (SW):

$$(^{134}\text{Cs}/^{137}\text{Cs})_{\text{SW}} = -0.011 + 3.98 \cdot 10^{-4} \cdot (\text{Latitude } ^\circ\text{N}) - 4.85 \cdot 10^{-5} \cdot (\text{Longitude } ^\circ\text{E})$$

Goodness of fit statistics (Variable $^{134}\text{Cs}/^{137}\text{Cs}$ Surface water): $R^2 = 0.447$

Equation of the model for bottom water (BW):

$$(^{134}\text{Cs}/^{137}\text{Cs})_{\text{BW}} = -0.042 + 8.89 \cdot 10^{-4} \cdot (\text{Latitude } ^\circ\text{N}) - 9.37 \cdot 10^{-5} \cdot (\text{Longitude } ^\circ\text{E})$$

Goodness of fit statistics (Variable $^{134}\text{Cs}/^{137}\text{Cs}$ Bottom water): $R^2 = 0.913$

C4. ^{90}Sr activity concentration in seawater

The ^{90}Sr activity concentration in seawater along the route of the Tundra expedition is shown in **figures 5-13a** and **b** respectively. In surface water the ^{90}Sr activity concentration range from 2 to 4 $\text{Bq}\cdot\text{m}^{-3}$. Maximum values about 3.5 $\text{Bq}\cdot\text{m}^{-3}$ were found between 100-140 $^\circ\text{E}$. But east of 150 $^\circ\text{E}$, the values decreased to about 0.5 $\text{Bq}\cdot\text{m}^{-3}$ at 170 $^\circ\text{E}$.

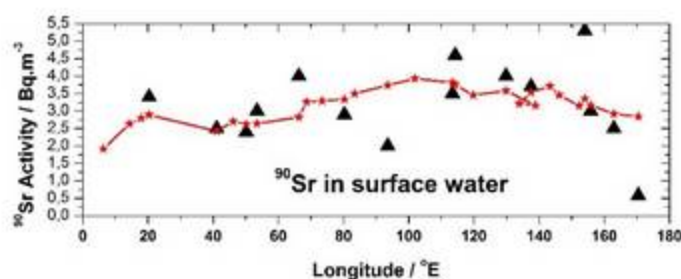


Figure 5-12a Longitudinal distribution of the ^{90}Sr activity concentration in surface seawater along the route of Tundra expedition. Predicted values in read

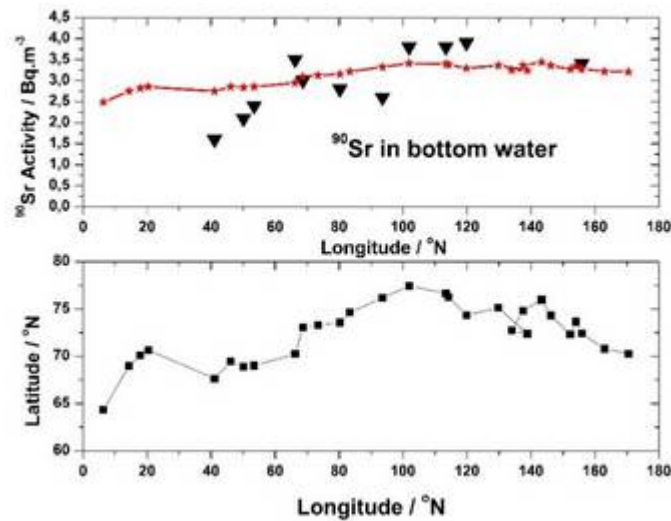


Figure 5-12b Longitudinal distribution of the ^{90}Sr activity concentration in surface and bottom seawater along the route of Tundra expedition. Predicted values in read

In bottom water the ^{90}Sr activity concentration range from 1.5 at 40 °E to maximum values about 4 $\text{Bq}\cdot\text{m}^{-3}$ between 100-120 °E.

Equation of the PLS model for ^{90}Sr activity concentration in Surface water (SW):

$${}^{\text{SW}}C_{90\text{Sr}} = -7.910 + 0.153 \cdot (\text{Latitude}^{\circ}\text{N}) + 9.6 \cdot 10^{-5} \cdot (\text{Longitude}^{\circ}\text{E}); [\text{Bq}\cdot\text{m}^{-3}]$$

Goodness of fit statistics: $R^2 = 0.16$

Equation of the PLS model ^{90}Sr activity concentration in Bottom Water (BW):

$${}^{\text{BW}}C_{90\text{Sr}} = -0.873 + 0.052 \cdot (\text{Latitude}^{\circ}\text{N}) + 0.0025 \cdot (\text{Longitude}^{\circ}\text{E}); [\text{Bq}\cdot\text{m}^{-3}]$$

Goodness of fit statistics: $R^2 = 0.21$

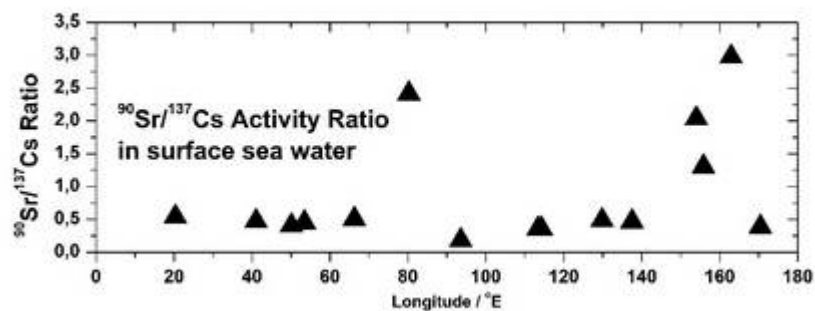


Figure 5-13a Longitudinal distribution of the $^{90}\text{Sr}/^{137}\text{Cs}$ activity ratio in surface seawater along the route of Tundra expedition.

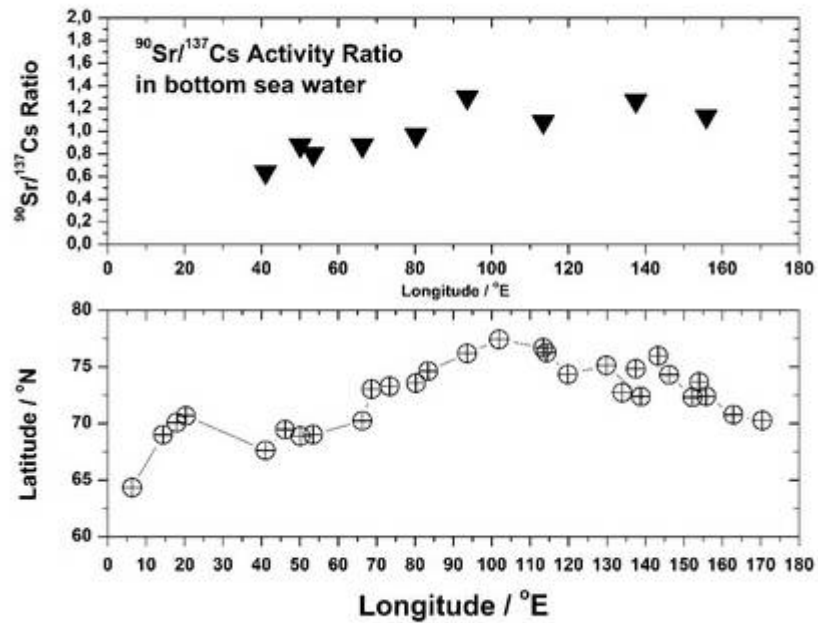


Figure 5-13b Longitudinal distribution of the $^{90}\text{Sr}/^{137}\text{Cs}$ activity ratio in bottom seawater and the route of Tundra expedition.

C5. ^{129}I concentration in seawater

The ^{129}I concentration in sea-water along the route of the Tundra expedition is shown in Figure 5-14. The concentration decrease from about $20 \cdot 10^{11}$ atoms. l^{-1} ($2 \cdot 10^{15}$ atoms. m^{-3}), ≈ 3 picomolar, to about $1 \cdot 10^{11}$ atoms. l^{-1} east of 160 °E.

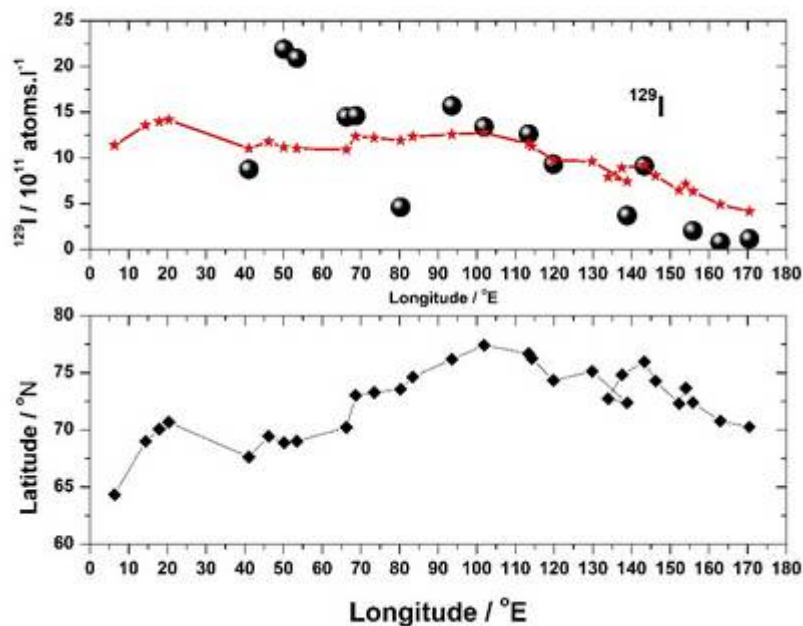


Figure 5-14 Longitudinal distribution of ^{129}I concentration in surface seawater and the route of Tundra expedition. Predicted values in read.

PLS Model parameters for ^{129}I concentration in surface seawater :

$${}^{\text{SW}}\text{C}_{129\text{I}} = -25.529 + 0.580 \cdot (\text{Latitude } ^\circ\text{N}) - 0.065 \cdot (\text{Longitude } ^\circ\text{E}); [10^{14} \text{ atoms.m}^{-3}]$$

Goodness of fit statistics: $R^2 = 0.311$

C6. $^{239+240}\text{Pu}$ activity concentration in seawater

The $^{239+240}\text{Pu}$ activity concentration in surface and bottom seawater along the route of Tundra expedition are given in **Figure 3-15a** and **b** respectively. In surface seawater the $^{239+240}\text{Pu}$ activity concentration decrease from about 10 mBq.m^{-3} to about 1 mBq.m^{-3} east of 160°E .

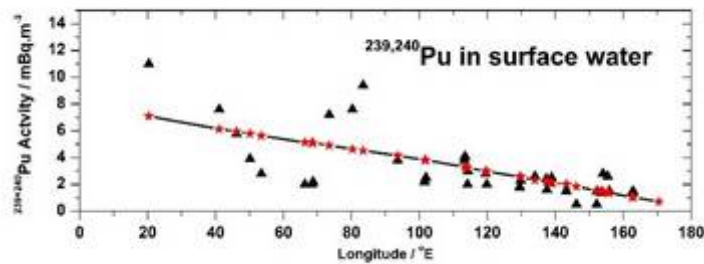


Figure 5-15a.

$^{239+240}\text{Pu}$ activity concentration in surface seawater along the route of Tundra expedition. Predicted values in red.

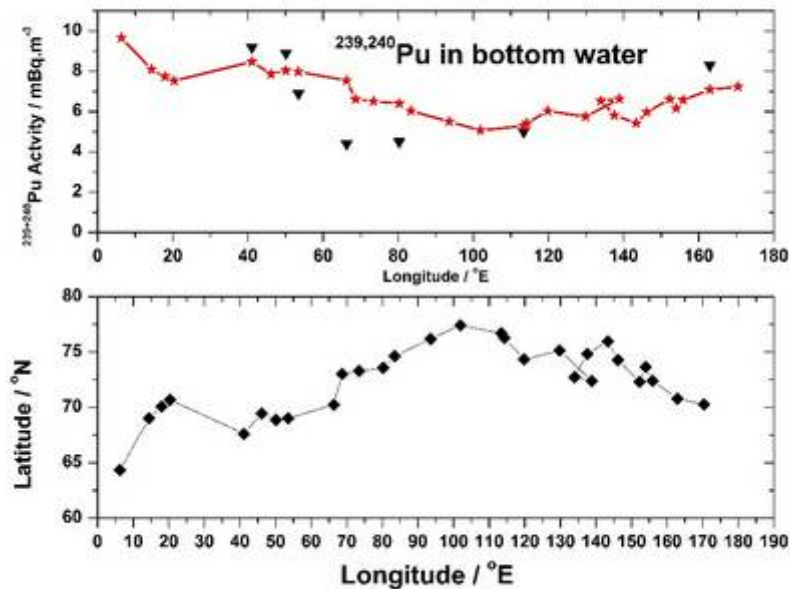


Figure 5-15b.

$^{239+240}\text{Pu}$ activity concentration in bottom seawater and the route of Tundra expedition.

In bottom seawater the $^{239+240}\text{Pu}$ activity concentration is more evenly distributed between $10 - 4 \text{ mBq.m}^{-3}$, with the minimum at $60\text{-}80^\circ\text{E}$ and maxima at 40°E and 160°E .

Equation of the model PLS model for activity concentration of $^{239,240}\text{Pu}$ in Surface water (SW):

$${}^{\text{SW}}C_{239,240\text{Pu}} = 5.948 + 0.028 \cdot (\text{Latitude}^{\circ}\text{N}) - 0.043 \cdot (\text{Longitude}^{\circ}\text{E}) ; [\text{mBq}\cdot\text{m}^{-3}]$$

Goodness of fit statistics (Variable ${}^{\text{SW}}C_{239,240\text{Pu}}$): $R^2 = 0.471$

Equation of the PLS model for $^{239,240}\text{Pu}$ Bottom water (BW):

$${}^{\text{BW}}C_{239,240\text{Pu}} = 30.96 - 0.331 \cdot (\text{Latitude}^{\circ}\text{N}) - 0.0028 \cdot (\text{Longitude}^{\circ}\text{E}) ; [\text{mBq}\cdot\text{m}^{-3}]$$

Goodness of fit statistics (Variable ${}^{\text{BW}}C_{239,240\text{Pu}}$): $R^2 = 0.432$

C7. ^{137}Cs and $^{239+240}\text{Pu}$ activity concentration in sediment

The integrated sediment activity of $^{239+240}\text{Pu}$ was measured in samples taken at sampling sites specified in **Table 5-3**, and the results are displayed in **Figure 5-16a** and **b**.

Table 5-3

Sampling location and integrated sediment activity of ^{137}Cs and $^{239+240}\text{Pu}$ at the Tundra

Station	Latitude		Longitude		Water depth m	Activity penetration depth cm	^{137}Cs [Bq/m ²]	$^{239+240}\text{Pu}$		
	°N	min	°E	SD				SD		
9	70	14	66	17	20	19	556	67	28.8	3.3
14	76	11	93	34	55	8	217	11		
18	75	8	129	50	58	9	393	17		
21	74	50	137	32	20	14	836	60	34.3	3.4
28	70	16	170	26	30	7	119	8	4.94	0.4

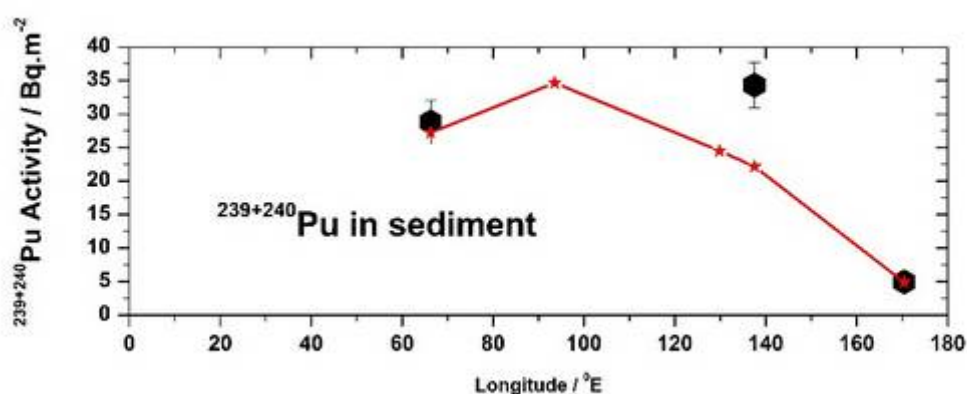


Figure 5-16a

Measured and predicted, integrated sediment activity of $^{239+240}\text{Pu}$ at specific sampling stations (see below). Predicted values in red

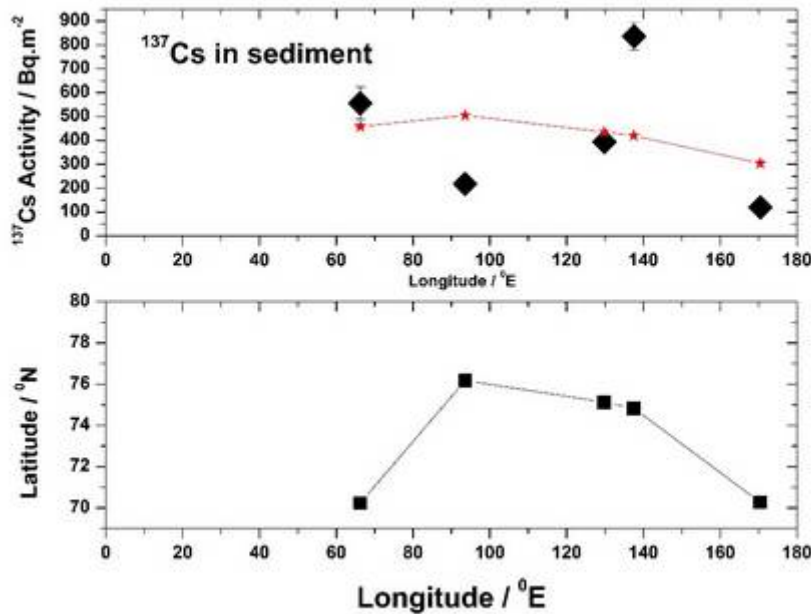


Figure 5-16

Measured and predicted integrated sediment activity of ^{137}Cs at specific sampling stations, given in the bottom diagram with latitude versus longitude. Predicted values in read

Equation of the model for predicted integrated sediment activity, $^{\text{SED}}A$, of $^{239+240}\text{Pu}$ [Bq/m²] in sediment:

$$^{\text{SED}}A_{239+240\text{Pu}} = -115.2 - 0,215 \cdot (\text{Longitude}^{\circ}\text{E}) + 2.23 \cdot (\text{Latitude}^{\circ}\text{N})$$

Goodness of fit statistics ($^{\text{SED}}A_{239+240\text{Pu}}$): $R^2 = 0,852$

Equation of the PLS model for predicted integrated sediment activity, $^{\text{SED}}A$, of ^{137}Cs [Bq.m⁻²] in sediment (SED):

$$^{\text{SED}}A_{137\text{Cs}} = -473.3 - 1.486 \cdot (\text{Longitude}^{\circ}\text{E}) + 14.66 \cdot (\text{Latitude}^{\circ}\text{N}); [\text{Bq}\cdot\text{m}^{-2}]$$

Goodness of fit statistics (Variable ^{137}Cs [Bq/m²]): $R^2 = 0.069$

D. Discussions

D1. Beryllium-7 activity concentrations in the Arctic air

The activity-concentration of ^7Be in air in the Arctic air as summarized in **Table 5-4** varies between 2 - 4.9 mBq.m⁻³ with average 2.8 ± 0.3 mBq.m⁻³ (Buraglio et al., 2001, Kulan, 2006, Paatero and Hatakka, 2000, Baskaran and Shaw, 2001, Dibb and Jaffrezo, 1993). The average of ^7Be activity concentration in air over the Arctic Ocean was, however, only about 0.6 mBq.m⁻³. In contrast the activity concentration of ^7Be in air close to the Siberian coast-line as high as 11 mBq.m⁻³ (Persson, 2013).

Table 5-4. Summary of atmospheric ⁷Be concentrations in Arctic and sub-Arctic air

Time	Location	Lat		Long		Be-7		Reference
		N+; S-	E+; W-	Arithm. Mean	SD	mBq.m ⁻³		
910728-0906	Arctic Ocean	82.07	51.00	0.62	0.52	This work ^{*)}		
910907-1004	Arctic Ocean	84.36	-2.32	0.51	0.33	This Work ^{*)}		
940605-0908	N Siberian coast	71	84	11.4	9.0	This work ^{*)}		
2000	Uppsala. Sweden	59.88	17.63	4.7	2.3	(Buraglio et al., 2001)		
1972-1995	Sweden	59.88	17.63	4.8	2.4	(Buraglio et al., 2001)		
1972-2003	Sweden. Kiruna	67.84	20.34	1.9	1.0	(Kulan, 2006)		
1972-2003	Sweden. Grindsjön	59.07	17.82	2.3	1.2	(Kulan, 2006)		
1972-2003	Sweden. Ljungbyhed	56.08	13.23	2.5	1.3	(Kulan, 2006, Aldahan et al., 2008)		
1995- 1997	Finland Sodankyla	67.37	26.65	2.5	2.0	(Paatero, 2000)		
1996	Alaska USA:Poker Flat	65.13	-147.48	3.0	2.0	(Baskaran and Shaw, 2001)		
1996	Alaska USA Eagle	65.9	-141.20	2.2	1.0	(Baskaran and Shaw, 2001)		
1988-1989	Dye3	65.18	43.82	2.6	1.1	(Dibb and Jaffrezo, 1993)		
1988-1990	Barrow	71.30	-156.77	1.9	1.1	(Dibb and Jaffrezo, 1993)		
1988-1991	Kap Toban	70.42	-21.97	2.4	1.3	(Dibb and Jaffrezo, 1993)		
1988-1992	Nord	81.36	-16.40	2.5	1.4	(Dibb and Jaffrezo, 1993)		
1988-1993	Thule	77.50	-69.33	3.7	1.9	(Dibb and Jaffrezo, 1993)		
1997-2004	Summit. Greenland	72.575	-27.55	2.0	0.5	(Dibb, 2007)		

^{*)}(Persson, 2013).

D2. ²¹⁰Pb activity concentrations in the Arctic air

Observations of the activity concentration of ²¹⁰Pb in the air over the Arctic ocean as summarized in **Table 5-5**, varies between 37 – 176 μBq.m⁻³ (Persson and Holm, 2013, McNeary and Baskaran, 2003, Dibb and Jaffrezo, 1993, Dibb, 2007, Paatero et al., 2003, Samuelsson et al., 1986). In 1991 we found the average activity concentration of ²¹⁰Pb over the Arctic Ocean to be 40±4 μBq.m⁻³. In the air close to land masses the activity concentration of ²¹⁰Pb in the air increase to 269- 2712 μBq.m⁻³ (McNeary and Baskaran, 2003, Baskaran and Shaw, 2001, Dibb and Jaffrezo, 1993); with the highest values of about 2500 μBq.m⁻³ at the Siberian coastline (Persson and Holm, 2013).

Table 5-5. Activity concentrations (μBq.m⁻³) of ²¹⁰Pb recorded at different locations during the Tundra-94 expedition.

Time	Location	Lat		Long		Pb-210		Po-210		Reference
		°N	°E	Average	SD	Average	SD	μBq.m ⁻³		
940605>0703	Siberian Tundra	71	84	2373	364	2044	870	This work		
940704>0908	Siberian Tundra	71	84	2712	1079	2336	994	This work		

D3. ^{137}Cs activity distribution

The minimum values of the ^{137}Cs activity concentration water along the route of the Tundra were found in South-eastern Barents Sea: 5.3 Bq.m^{-3} of surface-water, and of bottom-water 6.4 Bq.m^{-3} . Maximum values were found in the Western Laptev sea: 12.8 Bq.m^{-3} of surface-water, and of bottom-water 5.1 Bq.m^{-3} .

East of 150°E the $^{134}\text{Cs} / ^{137}\text{Cs}$ ratios are less than 0.003, indicating that less than 6% of the ^{137}Cs originated from the Chernobyl accident.

The $^{134}\text{Cs} / ^{137}\text{Cs}$ activity ratio of 0.014 in the freshwater indicates that the Chernobyl component in the river systems is the same (30%) as in the marine waters.

D4. ^{90}Sr activity distribution

The relative magnitudes of ^{90}Sr inputs to the Arctic Ocean differ from those for ^{137}Cs for the same sources. The $^{137}\text{Cs}/^{90}\text{Sr}$ activity ratio of 35 reported for Chernobyl fallout was sufficiently high that ^{90}Sr inputs from this source can be considered to be negligible (Aarkrog, 1988). The present fallout concentration in the oceans is assumed to be about 1.6 Bq/m^3 (Dahlgard, 1995). Sellafield represents a major ^{90}Sr source term, which similar to ^{137}Cs , attained a maxima in the late 1970's and has decreased substantially since that time. An important additional source of ^{90}Sr to the Siberian seas is associated with river runoff from fallout, discharges from nuclear reprocessing plants and inputs from accidental releases of ^{90}Sr , such as the Khystym accident on 29 September 1957 at Mayak, USSR (Lollino et al., 2014). The greater mobility of ^{90}Sr compared to ^{137}Cs in freshwater environments results in reduced ^{90}Sr residence times in soils and more rapid transport through the drainage basin to marginal seas. By using the record of reported ^{90}Sr discharges, transport times of less than 10 y and transfer factors of 10 Bq.m^{-3} per PBq.a^{-1} the Sellafield contribution to Barents Sea water is estimated to be approximately 0.5 Bq.m^{-3} in 1994 (Gray et al., 1995). The addition of a fallout component of approximately 1.6 Bq.m^{-3} is not sufficient to give the values ($> 3 \text{ Bq.m}^{-3}$) measured in the Kara and Laptev Seas. These results suggest an additional contribution of the order of $1\text{-}2 \text{ Bq.m}^{-3}$ to ^{90}Sr concentrations on the Siberian shelves. Contributions from riverine sources will generally only play a minor role since most the salinities are too high.

The $^{90}\text{Sr}/^{137}\text{Cs}$ fallout ratio in seawater is approximately 0.7 while Sellafield discharge results give an average cumulative decay corrected $^{90}\text{Sr}/^{137}\text{Cs}$ ratio of 7 between 1980 and 1992 (Gray et al., 1995, Dahlgard et al., 1995). The measured $^{90}\text{Sr}/^{137}\text{Cs}$ (non-Chernobyl) ratios in surface water (**Figure 5-13**) are also close to a value of 0.14 over a wide range of stations from the Barents to the Laptev Seas, despite the observation above that much of this signal is from Sellafield. Clearly, the ^{90}Sr input from the Russian river systems has been sufficiently large to reduce the $^{137}\text{Cs}/^{90}\text{Sr}$ activity ratio to values similar to fallout levels. Bottom waters show slightly higher ratios indicating a Sellafield contribution. Calculations as above applying known transfer factors and transport times reveal, however, that direct transport will not notably effect the fallout ratio. Instead the Sellafield activity must be of an older date, reflecting a longer half-life on the shelf than expected, or recirculated from the central Arctic Ocean.

D5. ^{129}I distribution

The decreasing gradient in ^{129}I activity, east of the Barents Sea to the Laptev Sea, reflects the general increase in ^{129}I discharges since the 1980's. The sharp decrease in ^{129}I concentrations at 150 °E indicates that the front between Atlantic and Pacific origin water has been encountered. In the 1980s, this front was located over the Lomonosov Ridge, but has shifted to its present position over the Mendelyev Ridge (McLaughlin et al., 1996, Smith et al., 1998). The relatively low radionuclide levels measured in the East Siberian Sea are typical of fallout values associated with Pacific-origin water transported into this region from the Bering Sea.

D6. $^{239+240}\text{Pu}$ activity distribution

Plutonium activity concentrations and isotopic ratios, measured along the Siberian Shelf and in the Central Arctic Ocean, indicate that it mainly originates from global fallout of atmospheric nuclear weapons tests. This demonstrate that plutonium fallout of atmospheric nuclear weapons tests, deposited at mid-latitudes in the North Atlantic in the late-1950s and early-1960s, have found their way to the Arctic interior and beyond (Kershaw and Baxter, 1995, Josefsson, 1998);Herrmann, 1998 #473}.

Measured $^{238}\text{Pu}/^{239,240}\text{Pu}$ activity ratios in the water column yield no evidence of any leakage of plutonium from dumped nuclear wastes in the Kara and Barents Seas. Were leakage of plutonium to occur in the future from dumped nuclear wastes in the Kara and Barents Seas, it is likely that some of it will be transported through the Eurasian Shelf and into the Central Arctic with the Transpolar Drift, on a timescale of one to two decades, eventually exiting the Arctic through Fram Strait.

The geographical distribution of plutonium indicate that a broad peak that appears to have passed through the North Pole recently. We attribute this peak to the plutonium 'signal' that entered the Arctic following the period of maximal fallout deposition referred to above. The distribution is consistent with the well-established pattern of water-mass circulation in the Arctic, bearing in mind the limited number of plutonium observations available.

E. References

- AARKROG, A. 1988. The radiological impact of the Chernobyl debris compared with that from nuclear-weapons fallout. *Journal of Environmental Radioactivity*, 6, 151-162.
- ALDAHAN, A., HEDFORS, J., POSSNERT, G., KULAN, A., BERGGREN, A. M. & SODERSTROM, C. 2008. Atmospheric impact on beryllium isotopes as solar activity proxy. *Geophysical Research Letters*, 35.
- BASKARAN, M. & SHAW, G. E. 2001. Residence time of arctic haze aerosols using the concentrations and activity ratios of Po-210, Pb-210 and Be-7. *Journal of Aerosol Science*, 32, 443-452.
- BURAGLIO, N., ALDAHAN, A., POSSNERT, G. & VINTERSVED, I. 2001. I-129 from the nuclear reprocessing facilities traced in precipitation and runoff in northern Europe. *Environmental Science & Technology*, 35, 1579-1586.
- CARLSON, L. & HOLM, E. 1992. Radioactivity in Fucus-vesiculosus l from the baltic sea following the Chernobyl accident. *Journal of Environmental Radioactivity*, 15, 231-248.
- DAHLGAARD, H. 1995. Transfer of European coastal pollution to the Arctic - Radioactive-tracers. *Marine Pollution Bulletin*, 31, 3-7.
- DAHLGAARD, H., CHEN, Q., HERRMANN, J., NIES, H., IBBETT, R. D. & KERSHAW, P. J. 1995. On the background level of Tc-99, Sr-90 and Cs-137 in the North-Atlantic. *Journal of Marine Systems*, 6, 571-578.

- DIBB, J. E. 2007. Vertical mixing above Summit, Greenland: Insights into seasonal and high frequency variability from the radionuclide tracers Be-7 and Pb-210. *Atmospheric Environment*, 41, 5020-5030.
- DIBB, J. E. & JAFFREZO, J. L. 1993. Beryllium-7 and Pb-210 in aerosol and snow in the Dye-3 gas, aerosol and snow sampling program. *Atmospheric Environment Part a-General Topics*, 27, 2751-2760.
- GRAY, J., JONES, S. R. & SMITH, A. D. 1995. Discharges to the environment from the Sellafield site, 1951-1992. *Journal of Radiological Protection*, 15, 99-131.
- JOSEFSSON, D. 1998. *Atropogenic Radionuclides in the Arctic Ocean. Distributin and pathways*. PhD thesis LUNFD06/(NFRA-1036)/1-159/1998, Lund University, Sweden.
- KERSHAW, P. & BAXTER, A. 1995. The transfer of reprocessing wastes from north-west Europe to the arctic. *Deep-Sea Research Part Ii-Topical Studies in Oceanography*, 42, 1413-1448.
- KULAN, A. 2006. Seasonal Be-7 and Cs-137 activities in surface air before and after the Chernobyl event. *Journal of Environmental Radioactivity*, 90, 140-150.
- LOLLINO, G., ARATTANO, M., GIARDINO, M., OLIVEIRA, R., SILVIA, P. & EDS.. 2014. *Engineering Geology for Society and Territory: Education, professional ethics and public recognition of engineering geology, Volume 7.*, Springer.
- MCLAUGHLIN, F. A., CARMACK, E. C., MACDONALD, R. W. & BISHOP, J. K. B. 1996. Physical and geochemical properties across the Atlantic Pacific water mass front in the southern Canadian Basin. *Journal of Geophysical Research-Oceans*, 101, 1183-1197.
- MCNEARY, D. & BASKARAN, M. 2003. Depositional characteristics of Be-7 and Pb-210 in southeastern Michigan. *Journal of Geophysical Research-Atmospheres*, 108, 15.
- MITCHELL, N. T. & STEELE, A. K. 1988. The marine impact of Cesium-134 and Cesium-137 from the Chernobyl reactor accident. *Journal of Environmental Radioactivity*, 6, 163-175.
- PAATERO, J. 2000. Wet deposition of radon-222 progeny in northern Finland measured with an automatic precipitation gamma analyser. *Radiation Protection Dosimetry*, 87, 273-280.
- PAATERO, J. & HATAKKA, J. 2000. Source areas of airborne Be-7 and Pb-210 measured in Northern Finland. *Health Physics*, 79, 691-696.
- PAATERO, J., HATAKKA, J., HOLMEN, K., ENEROTH, K. & VIISANEN, Y. 2003. Lead-210 concentration in the air at Mt. Zeppelin, Ny-Alesund, Svalbard. *Physics and Chemistry of the Earth*, 28, 1175-1180.
- PERSSON, B. R. R. 2013. Transfer analysis of ²¹⁰Pb. and ²¹⁰Po in the terrestrial environment. In: KARUNAKARA, N. & BASKARAN, M., eds. 2nd International Conferene of Po and Radioactive Pb Isotopes, 19-13 February 2013 2013 INCOPoPb-2013 conference, Mangalore University, India. Mangalore, India: Mangalore University, 44-47.
- PERSSON, B. R. R. & HOLM, E. 2013. ⁷Be. ²¹⁰Pb. and ²¹⁰Po in the surface air from the Arctic to Antarctica. *INCOPoPb-2013 conference, Mangalore University*.
- SAMUELSSON, C., HALLSTADIUS, L., PERSSON, B., HEDVALL, R., HOLM, E. & FORKMAN, B. 1986. Rn-222 and Pb-210 in the arctic summer air. *Journal of Environmental Radioactivity*, 3, 35-54.
- SMITH, J. N., ELLIS, K. M. & KILIUS, L. R. 1998. I-129 and Cs-137 tracer measurements in the Arctic Ocean. *Deep-Sea Research Part I-Oceanographic Research Papers*, 45, 959-984.
- VINTERSVED, I. 1994. Intercomparison of large stationary air samplers In: DAHLGAARD, H. (ed.) *Nordic Radioecology. The transfer of radionuclides through Nordic ecosystems to man*. Amsterdam: Elsevier Science B.V.